

See discussions, stats, and author profiles for this publication at: <https://www.researchgate.net/publication/308806575>

# A mixed-integer linear model for optimal operation of hybrid AC-DC microgrid considering Renewable Energy Resources and PHEVs

Conference Paper · June 2015

DOI: 10.1109/PTC.2015.7232507

---

CITATIONS

10

READS

113

4 authors, including:



Payam Teimourzadeh Baboli

OFFIS

27 PUBLICATIONS 355 CITATIONS

[SEE PROFILE](#)



M.-R. Haghifam

Tarbiat Modares University

392 PUBLICATIONS 6,208 CITATIONS

[SEE PROFILE](#)

Some of the authors of this publication are also working on these related projects:



Evaluating the Impacts of High Penetration of Electric Vehicles on Tehran Electric Energy Distribution Company's Servicing Area [View project](#)



Building block approach creates new metalloproteins [View project](#)

# A Mixed-Integer Linear Model for Optimal Operation of Hybrid AC-DC Microgrid Considering Renewable Energy Resources and PHEVs

P. Teimourzadeh Baboli

Assistant Professor in University of Mazandaran, Faculty of Engineering & Technology, Babolsar, Iran.

[pteimourzadeh@ieee.org](mailto:pteimourzadeh@ieee.org)

S. Bahramara

PhD student in Tarbiat Modares University, Faculty of Electrical and Computer Engineering, Tehran, Iran.

[s.bahramara@modares.ac.ir](mailto:s.bahramara@modares.ac.ir)

M. Parsa Moghaddam, M.-R. Haghifam

Professors in Tarbiat Modares University, Faculty of Electrical and Computer Engineering, Tehran, Iran.

[parsa@modares.ac.ir](mailto:parsa@modares.ac.ir), [haghifam@modares.ac.ir](mailto:haghifam@modares.ac.ir)

**Abstract**—The share of DC-based Renewable Energy Resources (RERs) and electricity storage systems are increasing due to developments of smart grid technologies. Moreover, the share of DC-based load has rapid growth due to significant developments of power electronic technologies. Therefore, a more flexible power system is required for efficient integration of emerging loads and generators. In this paper, hybrid AC-DC Microgrid (MG) is incorporated as an appropriate topology versus conventional AC MG to reinforce the integration of RERs and Plug-in Hybrid Electric Vehicles (PHEVs). A mixed integer linear model is developed for operation of both hybrid AC-DC MG and conventional AC MG topologies considering high penetration of RERs and PHEVs. This operation model is solved by GAMS optimization software to minimize the operation cost and find the optimum inter-resource scheduling in the day-ahead market. Numerical study is conducted to evaluate the ability of both topologies for better utilizing the opportunities of integration.

**Index Terms**— Conventional AC microgrid, energy efficiency, hybrid AC-DC microgrid, renewable energy resource, plug-in hybrid electric vehicle.

## I. NOMENCLATURE

### Indices:

|     |                                   |
|-----|-----------------------------------|
| $c$ | index of load point               |
| $i$ | index of contingency              |
| $k$ | index of PHEVs' discharging steps |
| $m$ | index of year                     |
| $n$ | index of PHEVs' number            |
| $t$ | index of hour                     |

### Parameters:

|                   |  |
|-------------------|--|
| $A$               | annualized cost  |
| $ACIT_i$          | average customer interruption frequency at load point $i$                  |
| $C_{O\&M}$        | operation and maintenance cost of DG (USD)                                 |
| $frac_{i,k}$      | fraction of the load which is lost at load point $i$ , for contingency $c$ |
| $HR$              | heat rate ( $kWh/m^3$ )  |
| $i_R$             | annual real interest rate (%)  |
| $Load_{AC}(t)$    | AC load at $t$ (kW)  |
| $Load_{DC}(t)$    | DC load at $t$ (kW)  |
| $Load_{Total}(t)$ | total load at $t$ (kW)   |
| $LPENS_i$         | energy not supplied of the load point $i$                                  |
| $P$               | present value  |
| $PR_{fuel}$       | fuel price (USD)   |
| $PR_{sell}$       | electricity selling price to grid (\$/kWh)                                 |
| $PR_{TOU}(t)$     | time-of-use rates at $t$ (\$/kWh)  |
| $P_PV(t)$         | generation of PV panel at $t$ (kW)   |
| $P_{WT}(t)$       | generation of wind turbine at $t$ (kW)                                     |
| $Pd_i$            | weighted average amount of power   |

$Pr_c$

$Ps_i$

$P_{conv}$

$PEV^n_{charge,max}$

$PEV^n_{dcharge,max}$

$P_{DG,max}$

$PG_{max}$

$RR$

$SOC^n_{min}$

$SOC^n(t^n_{arr})$

$SOC^n(t^n_{dep})$

$SOC^n_{in}$

$SOC^n_{out}$

$QEV^n$

$\alpha_{dcharge}^k$

$\eta_{AC/DC}$

$\eta_{DC/AC}$

$\eta_{DG}$

### Binary Variables:

$X_{AC/DC}(t)$

$X_{DC/AC}(t)$

$X^n_{charge}(t)$

$X^n_{dcharge}(t)$

$XG_{in}(t)$

$XG_{out}(t)$

### Variables:

$F(t)$

$P_{AC/DC}(t)$

$PEV^n_{charge}(t)$

$PEV^{n,k}_{dcharge}(t)$

$PEV^n_{dcharge}(t)$

$P_{DC/AC}(t)$

$P_{DG}(t)$

$PG_{in}(t)$

$PG_{out}(t)$

$SOC^n(t)$

disconnected

probability of occurrence of contingency  $c$   
weighted average amount of power shed at load point  $i$

rated power of converter (kW)

maximum charging power of  $n$ -th PHEV's battery (kW)

maximum discharging power of  $n$ -th PHEV's battery (kW)

maximum capacity of DG (kW)

maximum transmitted power through grid (kW)

ramp rate (kWh/h)

minimum state-of-charge of  $n$ -th PHEV's battery

state-of-charge of  $n$ -th PHEV's battery at arriving time

state-of-charge of  $n$ -th PHEV's battery at departure time

input state-of-charge of  $n$ -th PHEV's battery

output state-of-charge of  $n$ -th PHEV's battery

capacity of  $n$ -th PHEV's battery (kWh)

The coefficient of PHEVs' discharging steps

efficiency of rectifier (P.U.)

efficiency of inverter (P.U.)

efficiency of DG unit (P.U.)

consumption of natural gas at  $t$  (m<sup>3</sup>)

converted AC to DC power at  $t$  (kW)

charging power of  $n$ -th PHEV's battery at  $t$  (kW)

discharging power steps of  $n$ -th PHEVs' battery at  $t$  (kW)

discharging power of  $n$ -th PHEVs' battery at  $t$  (kW)

converted power from DC to AC at  $t$  (kW)

generation of DG at  $t$  (kW)

purchased power from external grid at  $t$  (kW)

delivered power to external grid at  $t$  (kW)

state-of-charge of battery at  $t$  (P.U.)

## I. INTRODUCTION

Widespread use of Renewable Energy Resources (RERs) in low voltage AC distribution networks is endorsed due to environmental, customers' security and grid's efficiency issues. New small generators with intermittent output power are entered in the distribution network. AC microgrids facilitate the connection of the mentioned resources with conventional AC distribution systems. Thus, the nature of generation portfolio is changing. Besides, load's observability and controllability are increased by developing smart grid technologies. Moreover, penetration of storage systems is also increasing in distribution level, e.g. batteries and plug-in hybrid electric vehicles (PHEVs). In such environment, strong integration of RERs and PHEVs is one of the main goals of power system planners. In this paper, inclusion of DC link is suggested as an appropriate solution for reinforcing the integration of the mentioned demand-side resources.

PHEVs provide several advantages for owners which lead to their increasing share in future transportation system. Moreover, their storages ability facilitates the integration of RERs into distribution network that is the most transformative impact on the power system. The literatures on this topic are mainly concentrated on investigation of wind and solar energy [1-6]. Besides, the concept of hybrid microgrid has been investigated as an economical, environmental friendly and efficient distribution grid of the future from different viewpoints [7-12]. Liu *et al* applied a centralized coordination control algorithm for smooth power transfer between AC and DC links [7, 8]. Although the controllability and predictability of centralized control methods are high in compare with decentralized control methods, the promptness and reliability of them are much fewer. Therefore, a system control failure may lead to total grid outage. A dynamic assessment of hybrid AC-DC system is investigated in Ref. [9]. Authors in [10] employed power consumption control with the droop characteristic and maintained the DC bus voltage within the acceptable range. In the latter study, the test system was consisted of a wind generator and several controllable loads with no controllable generators, e.g. DG unit, fuel cell, etc. Moreover, Ref. [10] did not investigate the stand-alone operation in contingency states. These studies are focused on power electronic aspects of the problem or the control framework of the system in a constant operating point.

This paper investigates the optimum operation of hybrid AC-DC Microgrid (MG) considering the time-dependence impacts of the network over 24 hours. Here, two different microgrid configurations are considered with the same amount of electricity consumption and local generation. Indeed, the important role of grid's configuration is investigated in this study. In the first configuration (conventional AC MG), there are three kinds of small-scale RERs (i.e. wind turbine, photovoltaic arrays and distributed generator), several PHEVs and the electricity load. All of them are connected to an AC distribution network and the extra/shortage of power is transmitted with the external grid. The second configuration (the proposed hybrid AC-DC MG) is consisted of all the mentioned resources and load with similar quantity. But, there is semi-separated AC and DC links that reinforces the integration of RERs and PHEVs to reduce the intermittency problem of RERs. Regarding this matter, the operation

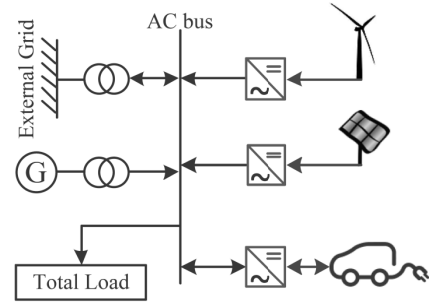


Fig. 1. Conventional AC LN.

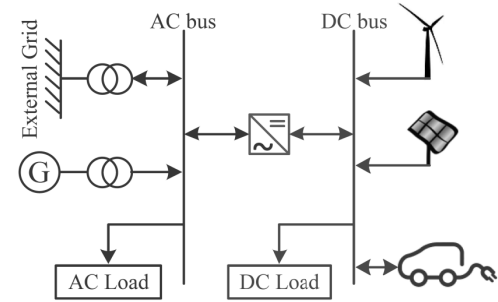


Fig. 2. Hybrid AC-DC LN.

frameworks of both configurations are modeled. The optimum solution of both configurations is compared with each other and the amount of efficiency improvement is demonstrated. The main contributions of the paper is proposing a mixed integer linear model for comparing the operation of hybrid AC-DC and conventional AC MGs considering the RERs and PHEVs to underline the impacts of the distribution network topology on the integration of RERs and PHEVs.

## II. TOPOLOGY DESCRIPTION

In this section, two different topologies are presented in details to model conventional AC and hybrid AC-DC MGs.

### a. Conventional AC Microgrid

The configuration of the AC MG is shown in Fig. 1. This MG is consisted of AC lines (buses), fossil-fuel-based generator (micro-turbine), RERs (wind turbine and photovoltaic arrays) and storage system (PHEVs) which serves an AC load. The power balance of the network is provided by power transactions with external grid.

### b. Hybrid AC-DC Microgrid

Hybrid AC-DC MG is proposed to reduce losses of multiple power conversions and to facilitate the connection of various AC and DC resources and loads. Operation problem of a hybrid MG is more complicated than conventional AC MGs. Fig. 2 illustrates the proposed hybrid AC-DC MG topology.

As shown in Fig. 2, in the hybrid MG, both DC and AC resources are incorporated in power generation. The main electricity power is injected from sub-transmission substation (external grid) to balance AC and DC loads and resources with the help of the main converter between AC and DC links.

## III. MATHEMATICAL FORMULATION

In the following, the mathematical formulation of both

conventional AC and hybrid AC-DC MG topologies are presented. The objective function is minimizing the overall operation cost over the entire scheduling period. The supply quantity of RERs are forecasted and considered as input data. Regarding this matter, the scheduling problem is to determine the supply quantity of DG unit, charge/discharge rate of the PHEVs and the amount of power transactions with external grid over 24 hours as formulated in the following:

$$OC = \sum_{t=1}^{24} \left[ PG_{in}(t) \times PR_{TOU}(t) - PG_{out}(t) \times PR_{sell} + \{F(t) \times PR_{fuel} + C_{O&M}\} + \sum_{n=1}^{10} \left( \left( \sum_{k=1}^3 PEV_{dch\ arg e}^{n,k}(t) \times PR_{TOU}(t) \times \alpha_{dch\ arg e}^k \right) \right) - PEV_{ch\ arg e}^n(t) \times PR_{TOU}(t) \right] \quad (1)$$

The first term of Eq. (1) determines the energy purchase cost from external grid when the total generation of MG resources is not adequate for serving its load. The second term represents the income from selling the extra amount of MG's generation to the external grid. The third term demonstrates the operation cost of DG unit that consists of fixed operating and maintenance costs and variable cost related to the consumption and price of the fuel. The forth term denotes the total cost of all PHEVs that consist of the cost of discharging the battery of PHEVs and the income from charging them. As it is indicated in Eq. (1), three charging steps is considered for discharging the batteries of PHEVs.

The constraints of both MG topologies are formulated as follows:

#### a. Conventional AC MG constraints:

##### 1. Power balance equation:

$$\begin{aligned} & \eta_{DC/AC} \left( P_{WT}(t) + P_{PV}(t) + \sum_{n=1}^N \sum_{k=1}^3 PEV_{dch\ arg e}^{n,k}(t) \right) \\ & + P_{DG}(t) + PG_{in}(t) = Load_{Total}(t) \\ & + \left( \sum_{n=1}^N PEV_{ch\ arg e}^n(t) \right) + PG_{out}(t) \end{aligned} \quad (2)$$

where  $Load_{Total}(t)$  is calculated by Eq. (3):

$$Load_{Total}(t) = Load_{AC}(t) + \frac{Load_{DC}(t)}{\eta_{AC/DC}} \quad (3)$$

The consumption of DC loads is measured while they are connected to the DC link. Thus, when these loads are supplied by AC voltage the rectifier's loss must be considered as it is indicated in Eq. (3).

##### 2. Constraints of DG unit operation:

- Constraint of maximum and minimum power of DG:

$$0 \leq P_{DG}(t) \leq P_{DG,max} \quad (4)$$

- Constraints of ramp rates of DG:

$$0 \leq P_{DG}(t) - P_{DG}(t+1) \leq RR \quad (5)$$

$$0 \leq P_{DG}(t+1) - P_{DG}(t) \leq RR \quad (6)$$

- Output power of DG unit:

$$P_{DG}(t) = F(t) \times HR \times \eta_{DG} \quad (7)$$

### 3. Constraints of PHEVs:

- Maximum charge/discharge rate constraints of the PHEVs:

$$0 \leq PEV_{ch\ arg e}^n(t) \leq X_{ch\ arg e}^n(t) \times PEV_{ch\ arg e,max} \quad (8)$$

$$0 \leq PEV_{dch\ arg e}^n(t) \leq X_{dch\ arg e}^n(t) \times PEV_{dch\ arg e,max} \quad (9)$$

where  $PEV_{dch\ arg e}^n(t)$  is calculated as following:

$$PEV_{dch\ arg e}^n(t) = \sum_{k=1}^3 PEV_{dch\ arg e}^{n,k}(t). \quad (10)$$

As it is indicated in Eq. (10) three discharge steps are considered based on the State-of-Charge (SOC) of the PHEVs' batteries. This kind of modeling increases the fairness of paying the remuneration schemes and prevents unnecessary deterioration of PHEV's battery.

Equation (11) determines the operation mode of the battery by defining two binary variables. By implying this constraints simultaneous occurrence of charging and discharging mode is prevented when the vehicle is in the parking. Moreover, it prevents any charging/discharging power of the PHEV's battery before arriving to or after departing from the parking.

$$\begin{cases} X_{ch\ arg e}^n(t) + X_{dch\ arg e}^n(t) \leq 1 & , t_{arr}^n \leq t \leq t_{dep}^n \\ X_{ch\ arg e}^n(t) = X_{dch\ arg e}^n(t) = 0 & , otherwise \end{cases} \quad (11)$$

#### • Constraints of discharging steps:

Constraint (12) depicts the limitation of the first discharging step and controls the discharging power of step 1 when  $0.7 \leq SOC^n(t) \leq 1$ .

$$0 \leq PEV_{dch\ arg e}^{n,1}(t) \leq (SOC^n(t) - 0.7) \times QEV^n \quad (12)$$

Constraint (13) depicts the limitation of the second discharging step and controls the discharging power of step 2 when  $0.4 \leq SOC^n(t) < 0.7$ .

$$\begin{cases} 0 \leq PEV_{dch\ arg e}^{n,2}(t) \leq (SOC^n(t) - 0.4) \times QEV^n \\ 0 \leq PEV_{dch\ arg e}^{n,2}(t) \leq (0.7 - 0.4) \times QEV^n \end{cases} \quad (13)$$

Constraint (14) depicts the limitation of the third discharging step and controls the discharging power of step 3 when  $0.2 \leq SOC^n(t) < 0.4$ .

$$\begin{cases} 0 \leq PEV_{dch\ arg e}^{n,3}(t) \leq (SOC^n(t) - 0.2) \times QEV^n \\ 0 \leq PEV_{dch\ arg e}^{n,3}(t) \leq (0.4 - 0.2) \times QEV^n \end{cases} \quad (14)$$

#### • Constraints of SOC:

The  $SOC$  of PHEV's battery constraint is formulated in (15). As it is shown in Eq. (16), the amount of SOC in each time step is calculated as follows:

$$SOC_{min}^n \leq SOC^n(t) \leq 1 \quad (15)$$

$$SOC^n(t+1) =$$

$$SOC^n(t) + \frac{PEV_{ch\ arg e}^n(t) - PEV_{dch\ arg e}^n(t)}{QEV^n} \quad (16)$$

Equations (17) and (18) fix the amount of PHEV's SOC in the arrival to and departure time from the parking, respectively.

$$SOC^n(t_{arr}^n) = SOC_{in}^n \quad (17)$$

$$SOC^n(t_{dep}^n) = SOC_{out}^n \quad (18)$$

#### 4. Constraints of trading with the grid:

Equations (19)-(21) address the constraints of bidirectional power transmission between MG and external grid.

$$0 \leq PG_{in}(t) \leq X_{in}(t) \times PG_{max} \quad (19)$$

$$0 \leq PG_{out}(t) \leq X_{out}(t) \times PG_{max} \quad (20)$$

$$X_{in}(t) + X_{out}(t) \leq 1 \quad (21)$$

#### b. Hybrid AC-DC MG constraints:

Unlike conventional AC MG, there are two power balance equations in hybrid AC-DC MG both in AC and DC buses.

##### 1. Power balance at AC bus:

$$\begin{aligned} P_{DG}(t) + PG_{in}(t) + (P_{DC/AC}(t) \times \eta_{DC/AC}) \\ = Load_{AC}(t) + PG_{out}(t) + P_{AC/DC}(t) \end{aligned} \quad (22)$$

##### 2. Power balance at DC bus:

$$\begin{aligned} P_{WT}(t) + P_{PV}(t) + \sum_{n=1}^N \sum_{k=1}^3 PEV_{charge}^{n,k}(t) \\ + (P_{AC/DC}(t) \times \eta_{AC/DC}) = Load_{DC}(t) \\ + \left( \sum_{n=1}^N PEV_{charge}^n(t) \right) + P_{DC/AC}(t) \end{aligned} \quad (23)$$

#### 3. Constraints of converter:

As described in the section 2, the role of converter is to perform the power balance in DC link. Equations (24)-(26) present the constraints of the mentioned converter.

$$P_{AC/DC}(t) \leq X_{AC/DC}(t) \times P_{conv} \quad (24)$$

$$P_{DC/AC}(t) \leq X_{DC/AC}(t) \times P_{conv} \quad (25)$$

$$X_{AC/DC}(t) + X_{DC/AC}(t) \leq 1 \quad (26)$$

#### 4. Other constraints

Additional constraints (4)-(21) of conventional AC MG are valid for the hybrid AC-DC MG.

## IV. NUMERICAL STUDY

In this study, a four-story university building [13], is considered as the case study to evaluate the effectiveness of the proposed methodology. The main electrical equipment of the building are as follows: air-conditioning, lighting, computers and laboratory appliances. Both AC and DC parts of the electricity load of the proposed system are illustrated in Fig. 3. The existing electricity resources of the case study are: 40 kW DG unit, 25 kW wind turbine and 25 kW PV arrays. Ten vehicles traffic to the parking lot with same battery storage capacity of 5 kWh. The considered arrival/departure time and the corresponding SOCs are listed in Table I. Moreover, the described MG is connected to external grid to balance its shortage/extral power up to 20 kW. The additional required data is summarized in Table II. The price of natural gas is considered 0.328 USD/m<sup>3</sup> [14]. The selling price (spot price) and time-of-use rates are shown in Fig. 4 [14].

The mentioned model is solved by GAMS software using CPLEX solver. Figs. 5 and 6 illustrate the operation results of

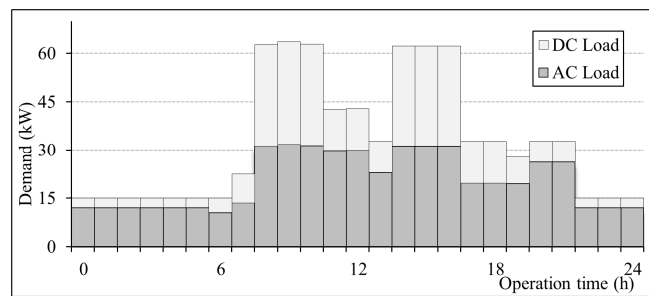


Fig. 3. The AC and DC share of the total electricity load.

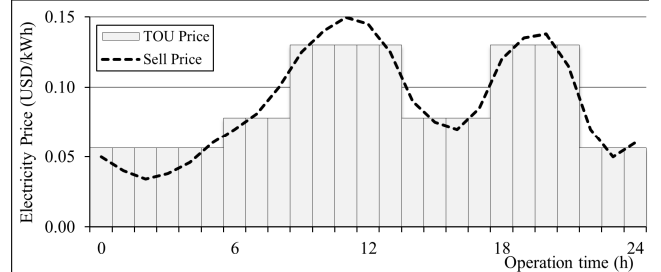


Fig. 4. The electricity exchange prices.

TABLE I. PHEVs' TRAFFIC DATA

| PHEV's no. | $t_{arr}$ (hr) | $t_{dep}$ (hr) | $SOC_{in}$ | $SOC_{out}$ |
|------------|----------------|----------------|------------|-------------|
| 1          | 7              | 20             | 0.8        | 0.8         |
| 2          | 8              | 18             | 0.2        | 1           |
| 3          | 8              | 17             | 0.5        | 0.9         |
| 4          | 9              | 14             | 0.8        | 0.3         |
| 5          | 9              | 17             | 0.4        | 1           |
| 6          | 9              | 17             | 0.35       | 0.9         |
| 7          | 9              | 18             | 0.5        | 0.9         |
| 8          | 10             | 18             | 0.7        | 0.7         |
| 9          | 10             | 19             | 0.85       | 0.3         |
| 10         | 11             | 20             | 0.4        | 0.9         |

TABLE II. ADDITIONAL REQUIRED DATA

| DG unit        | PHEV's battery              |                       |           |
|----------------|-----------------------------|-----------------------|-----------|
| $\eta_{DG}$    | 0.35                        | $QEV^n$               | 5 (kWh)   |
| $RR$           | 20 (kW/h)                   | $PEV_{charge,max}^n$  | 1.1 (kW)  |
| $C_{O\&M}$     | 0.03 (USD/h)                | $PEV_{dcharge,max}^n$ | 2.45 (kW) |
| $HR$           | 10.78 (kWh/m <sup>3</sup> ) | $SOC_{min}^n$         | 0.20      |
| Converter      |                             |                       |           |
| $P_{conv}$     | 40 (kW)                     |                       |           |
| $\eta_{AC/DC}$ | 0.90                        |                       |           |
| $\eta_{DC/AC}$ | 0.85                        |                       |           |

all MG's resources; namely output power of wind turbine, PV arrays, diesel generator, total charging power of PHEVs and injected power from the external grid for hybrid AC-DC and conventional AC MG, respectively. As it can be figured out from the results of two MGs the output power of DG unit in both networks follows spot prices to decrease the total operation costs of the system. Moreover, in high spot price periods (10:00 – 14:00 and 18:00 – 22:00), the power is transferred from MG to the external grid and on the other hand, in low spot price period the power is transferred from external grid to MG due to economical optimization.

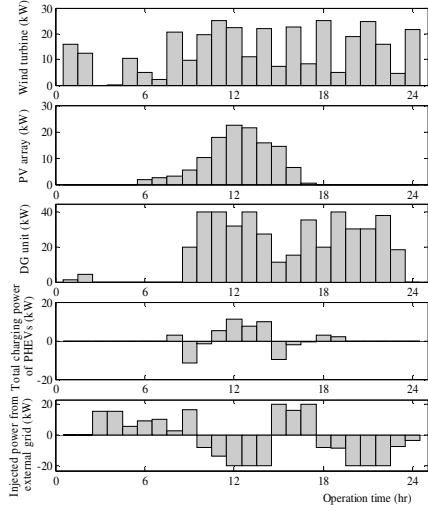


Fig. 5. Operation result of hybrid AC-DC MG.

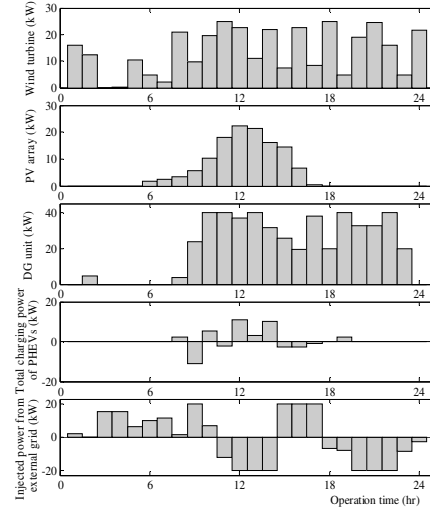


Fig. 6. Operation results of conventional AC MG

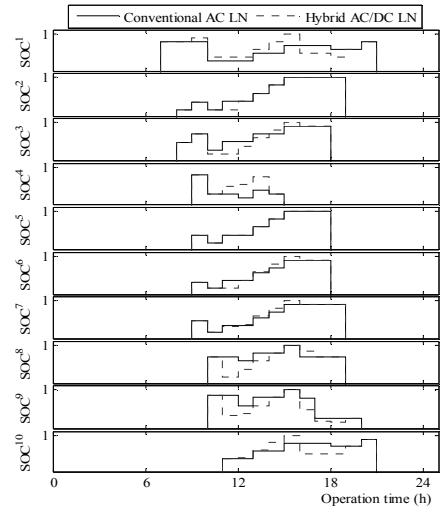


Fig. 7. Results of SOC variations in both MGs.

Fig. 7 depicts the variation of the SOC level of PHEV's batteries for hybrid AC-DC and conventional AC MG over the operation time. By focusing on Fig. 7, it can be seen that the number of various SOC levels is greater in hybrid AC-DC MG in compare with the conventional AC MG. Thus, PHEV's batteries in hybrid AC-DC MG are utilized more effectively which play a vital role in reducing the intermittency of RERs.

The final results over operation time for both hybrid AC-DC MG and conventional AC MG are presented in Table III. The total absorbed energy from the grid in hybrid AC-DC MG is decreased about 11.9 percent. Furthermore, total delivered energy to the grid in hybrid AC-DC MG is increased about 7.6 percent. It can be concluded that in the hybrid AC-DC MG, the flexibility of power exchange with the external grid and the opportunity of optimum utilization from the advantages of selling price variation is improved significantly.

The total natural gas consumption in hybrid AC-DC MG is decreased about 9 percent, due to two main reasons. First, in conventional AC MG the total load of the system is increased as a result of adding converters' losses as it was considered in Eq. 3. Second, batteries power exchange matches the generation of RERs with MG loads. Moreover, it can be noticed that the total operation cost in hybrid AC-DC MG is decreased about 23.8 percent.

## V. CONCLUSION

In this paper, two different topologies for microgrids (MGs) with multi AC and DC resources; namely conventional AC and hybrid AC-DC MG and loads were presented. In conventional AC MG, all AC and DC resources (DG unit, wind turbine, PV array and PHEVs) and loads are connected to a single AC link with separate converters. An additional DC link exists in hybrid AC-DC MG that all DC resources and loads can be connected to it directly. Since most of Renewable Energy Resources (RERs) produce DC power, hybrid AC-DC MGs will facilitate widespread use of these resources to meet emerging DC loads by reducing the intermittency of RERs through their integration with PHEVs. It can be concluded from the results of operation study that the operation cost can be reduced about 24 percent.

TABLE III. FINAL RESULTS OF OPERATION OVER 24 HOURS

|   | Microgrid Type |              |
|---|----------------|--------------|
|   | AC             | Hybrid AC-DC |
| Total Absorbed Energy from Grid (kWh)   | 149.1          | 131.3        |
| Total Delivered Energy to Grid (kWh)    | 157.9          | 169.9        |
| Total Natural Gas Consumption ( $m^3$ ) | 129.5          | 117.8        |
| Total operation cost (USD)              | 29.97          | 22.84        |

## REFERENCES

- [1] Q. Zhang, T. Tezuka, K. N. Ishihara, and B. C. McLellan, "Integration of PV power into future low-carbon smart electricity systems with EV and HP in Kansai Area, Japan," *Renewable Energy*, vol. 44, pp. 99-108, 2012.
- [2] V. Gass, J. Schmidt, and E. Schmid, "Analysis of alternative policy instruments to promote electric vehicles in Austria," *Renewable Energy*, vol. 61, pp. 96-101, 2012.
- [3] D. B. Richardson, "Electric vehicles and the electric grid: A review of modeling approaches, Impacts, and renewable energy integration," *Renewable and Sustainable Energy Reviews*, vol. 19, pp. 247-254, 2013.
- [4] S. M. Borba, A. Szklo, and R. Schaeffer, "Plug-in hybrid electric vehicles as a way to maximize the integration of variable renewable energy in power systems: The case of wind generation in northeastern Brazil," *Energy*, vol. 37, pp. 469-481, 2012.
- [5] D. Dallinger and M. Wietschel, "Grid integration of intermittent renewable energy sources using price-responsive plug-in electric vehicles," *Renewable and Sustainable Energy Reviews*, vol. 16, pp. 3370-82, 2012.
- [6] P. Teimourzadeh Baboli, M. Parsa Moghaddam, and F. Fallahi, "Utilizing Electric Vehicles on Primary Frequency Control in Smart power Grids," in *International Conference on Petroleum and Sustainable Development (ICPSD)*, 2011, pp. 1-5.
- [7] L. Xiong, W. Peng, and L. Pohchiang, "A hybrid AC/DC microgrid and its coordination control," *IEEE Trans. Smart Grid*, vol. 2, pp. 278-86, 2011.
- [8] W. Peng, L. Xiong, J. Chi, L. Pohchiang, and C. Fookhoong, "A hybrid AC/DC micro-grid architecture, operation and control," in *IEEE Power and Energy Society General Meeting*, 2011, pp. 1-8.
- [9] A. A. Radwan and Y.-R. Mohamed, "Assessment and mitigation of interaction dynamics in hybrid AC/DC distribution generation systems," *IEEE Trans. on Smart Grid*, vol. 3, pp. 1382-1393, 2012.
- [10] K. Kurohane, T. Senju, A. Uehara, A. Yona, T. Funabashi, and C.-H. Kim, "A hybrid smart AC/DC power system," in *5th IEEE Conference on Industrial Electronics and Applications (ICIEA)*, 2010, pp. 764-769.
- [11] P. Teimourzadeh Baboli, M. Shahparasti, M. P. Moghaddam, M. R. Haghifam, and M. Mohamadian, "Energy management and operation modelling of hybrid AC-DC microgrid," *IET Generation, Transmission & Distribution*, vol. 8, pp. 1700 – 1711, 2014.
- [12] P. Teimourzadeh Baboli, M. Moghaddam, M. Haghifam, M. Shafie-khah, and J. Catalão, "Serving Flexible Reliability in Hybrid AC-DC Microgrid using Demand Response and Renewable Energy Resources," *Power Systems Computation Conference (PSCC)*, 2014.
- [13] M. S. Ngan and C. W. Tan, "Assessment of economic viability for PV/wind/diesel hybrid energy system in southern Peninsular Malaysia," *Renewable and Sustainable Energy Reviews*, vol. 16, pp. 634-647, 2011.
- [14] X. Guan, Z. Xu, and Q.-S. Jia, "Energy-efficient buildings facilitated by microgrid," *IEEE Trans. on Smart Grid*, vol. 1, pp. 243-252, 2010.